Journal of Nano- and Electronic Physics
Vol. **13** No 6, 06012(6pp) (2021)

Журнал нано- та електронної фізики
Том **13** № 6, 06012(6cc) (2021)

On the Time Resolved Optogalvanic Spectroscopy of Neon in a Hollow Cathode Discharge

Koutayba Alnama*, Abdulkader Jazmati

Department of Physics, Atomic Energy Commission of Syria, P.O. Box 6091, Damascus, Syria

(Received 11 March 2021; revised manuscript received 10 December 2021; published online 20 December 2021)

Time resolved optogalvanic (OG) signals of $1s_4$-$2p_8$ (650.65 nm) and $1s_3$-$2p_7$ (653.29 nm) transitions have been studied in neon DC plasma. Numerical fit of the signals based on four-term rate equation model has been used to elucidate the contributions to the signal from four $1s_i$ levels. Evolution of decay rates of four $1s_i$ neon states as a function of discharge current has been studied. The dominant discharge processes for the first transition were photoionization and impact ionization, while for the second transition – the metastable-metastable collisional ionization mechanism was added to the previously mentioned mechanisms to produce the OG signal. The effective lifetimes of the $1s_i$ states have been determined for both transitions, where 2 μs is found for the resonance state $1s_2$, while the $1s_{3,4,5}$ have an almost equivalent effective lifetime of 40 μs. The long effective lifetime of all $1s_{2,4}$ states in comparison with their radiative lifetimes is attributed to the radiation trapping effect. The contribution of the $1s_i$ states to the OG signals has been studied. $1s_3$ state involvement was most important in the $1s_3$-$2p_7$ transition signal, while the $1s_4$ state has a large contribution to the $1s_4$-$2p_8$ transition signal.

Keywords*:* Optogalvanic, Effective lifetime, Neon, Plasma properties, Hollow cathode.

DOI: 10.21272/jnep.13(6).06012 PACS numbers: 62.23.Hj, 87.85.Dh

1. INTRODUCTION

Laser optogalvanic (OG) spectroscopy is a low cost, simple and sensitive technique to probe atomic transitions. It is used in a wide range of applications, including trace element detection [1], tunable dye laser calibration [2], plasma diagnostics [3], atomic and molecular spectroscopy [4], and plasma dynamics [5]. In a stationary state, a gas-discharge plasma contains atoms, molecules, ions, and free electrons. These species are in a dynamic equilibrium, which results in a defined impedance and subsequently a discharge current. Illumination of such a medium with radiation having a frequency corresponding to an atomic or molecular transition will perturb the equilibrium. Therefore, the discharge conductivity will change. This process is known as the OG effect.

Several theoretical and analytical approaches are suggested to understand the different processes contributing to the OG effect. These models are well described in [6]. Han et al. [7, 8] established an extended version of a mathematical rate equation model for the distribution of the excited state population of the species in a commercial hollow cathode discharge lamp. This model is based on the collisional ionization rate in the discharge plasma. According to this model, a four-term equation (expressing the first four $1s_i$ excited states) is used to fit the time-resolved OG signals of the $1s_i$-$2p_j$ transitions. Han et al. [7] used only two terms of the complete equation to fit the $1s_5$-$2p_9$ transition. In another work, Han et al. [8] used a three-term equation to obtain a reasonable fit for the $1s_4$-$2p_6$ transition. Mahmood et al. [9] described the $1s_5$-$2p_{9,4,5}$ transitions by a two-term equation. Piracha et al. [10] examined the $1s_5$-$2p_{6,7,8}$, $1s_4$-$2p_{6,7}$, $1s_3$-$2p_{2,5}$ and $1s_2$-$2p_{2,4,5}$ transitions. They found that the transitions $1s_2$-$2p_{2,4,5}$ can be fitted by a two-term equation, while those originating from $1s_5$ and $1s_4$ need a three-term equation to reproduce the experimental signals well.

The transitions arising from the metastable levels $1s_5$ and $1s_3$ show similar OG signals, while the signals originating from the $1s_2$ state are in opposite polarity to those from the metastable states [10]. Piracha et al. [6] studied the $1s_4$-$2p_{1\text{-}10}$ transitions and fitted them by a three-term equation. The temporal signals of the $2p_{7,8,10}$ transitions are found to have a double peak structure, which differs from the rest of the transitions, where a single peak is observed.

As it was mentioned by other groups [6-10], an error can occur in deducing and/or attributing the fitting parameters of the $1s_i$ states, such as the effective lifetime, in the case of a two- or three-term equation. The objective of this paper is to explore the time-resolved OG signal in more detail by using a four-term equation to get more accurate fitting parameters, such as effective lifetimes of the $1s_i$ states. In this paper, the time resolved OG signal of Ne is observed in a hollow cathode discharge lamp. A semi-empirical model is used to fit the associated time resolved OG signals with a four-term equation describing the four $1s_i$ states. Thereby, we could characterize more accurately the plasma medium in terms of collision effects and the population distribution of neutral and ionic species present in the discharge. This approach is based on a detailed experimental investigation and least-squares fitting of the time resolved OG signals of neon transitions.

2. EXPERIMENTAL

In the experimental setup, a dye laser (TDL 90) pumped by a Quantel Nd:YAG-laser (YG 980, 532 nm, 10 Hz) is used. The spectral and temporal widths of the laser pulse are about 0.05 cm^{-1} and 10 ns, respectively. A DCM laser dye was utilized to get the desired laser wavelengths. The dye laser beam was centered inside a commercial 1.5" diameter hollow cathode lamp (Herae-

* pscientific21@aec.org.sy

us, Yb-Ne) using a 5 mm diameter aperture.

The hollow cathode lamp pressure is less than 1 mbar, the cathode diameter is almost 1 cm, and it is operated through a regulated dc power supply (Type C610, Heraeus Noblelight). The current-limiting RC circuit consists of a 10 kΩ resistor and a 47 nF capacitor. A fraction of the laser beam (3 % of the laser pulse energy) is directed to the photodiode in order to trigger the oscilloscope (Tektronix TDS 3054 C). The OG signal is averaged 512 times for each transition and current value. The current dependent signals are measured in a 1.0 mA step.

3. THEORETICAL MODEL

The electronic configuration of the ground state of neon is $1s^22s^22p^6\ {}^1S_0$. The excited levels are well described by Racah coupling scheme [11]: $n\ell[K]J$, where ℓ is the orbital angular momentum of the external electron, K designates the angular momentum resulting from coupling of ℓ with the total angular momentum of the ion core, and J is the total angular momentum.

This coupling scheme defines the selection rule of the transitions among the excited states. For simplicity, Paschen notation can be used to describe the excited states where the configuration $1s^22s^22p^53s$ gives rise to four excited levels named $1s_5$, $1s_4$, $1s_3$ and $1s_2$, which correspond to the $3s[3/2]_2$, $3s[3/2]_1$, $3s'[1/2]_0$, $3s'[1/2]_1$ states, respectively. Following Racah notations, $1s_5$ and $1s_3$ represent two metastable states, while $1s_4$ is a semi-metastable and $1s_2$ is a resonant level with radiative lifetimes of 16 ns and 1.2 ns, respectively [12]. The $1s^22s^22p^53p$ configuration generates ten $2p_1$, $2p_2$, ..., $2p_{10}$ levels. The Racah notations of these states can be found in ref. [13]. According to Racah coupling scheme, these $2p_j$ levels can radiatively de-excite to at least one of the $1s_i$ levels and have typical radiative lifetimes of around 19 ns [14].

As the discharge environment is so complex, it is very hard to describe it by one theoretical model. To be able to give a quantitative understanding of the OG signal, all the processes involved in the discharge and their cross sections must be known. The use of the rate equation formalism to describe the different discharge processes can lead to a large number of equations, whose cross-section values are unavailable. Therefore, our characterization of a particular discharge is mainly experimental. Han's model is used in this work to get quantitative estimation of the collisional process rates in our gas discharge plasma.

As metastable states live longer than other states, the main process that maintains the discharge in dynamic equilibrium is the metastable-metastable collisional ionization $Ne^* + Ne^* \rightarrow Ne + Ne^+ + e^-$. In addition, photoionization of excited neon states by energetic photons $Ne^* + h\nu \rightarrow Ne^+ + e^-$ and electron impact ionization $Ne^{(*)} + e^- \rightarrow Ne^+ + 2e^-$ will also contribute to ionization.

After laser excitation of $1s_i$-$2p_j$ occurs, the excited $2p_j$ level will de-excite to the radiation-allowed $1s_i$ levels within the radiation lifetime of the $2p_j$ level, which, in turn, changes the population of the $1s_i$ levels. Therefore, the time resolved OG signal is an indirect estimation of the $1s_i$ population density and its decay rate. According to this model, the experimental time resolved OG signal could be expressed by the following expression:

$$\begin{aligned} S(t) = {} & \frac{a}{1-b\tau}[\exp(-bt) - \exp(-t/\tau)] + \\ & + \frac{c}{1-d\tau}[\exp(-dt) - \exp(-t/\tau)] + \\ & + \frac{e}{1-f\tau}[\exp(-ft) - \exp(-t/\tau)] + \\ & + \frac{g}{1-h\tau}[\exp(-ht) - \exp(-t/\tau)] \end{aligned} \quad (1)$$

where $S(t)$ is the OG signal, a, c, e and g are the amplitudes, b, d, f and h are the decay rates, τ represents the coupling between the temporal behavior of the discharge and the response of the electrical circuit used to extract the OG signal and can be defined empirically. The four terms in expression (1) represent the four $1s_i$ states. The $2p_j$ population will de-excite to the $1s_i$ states. In addition, only one of these amplitudes is negative to reflect a decrease in the population of the $1s_i$ state, in which laser excitation started.

The decay rates, as defined in the model, have a linear relationship with the discharge current I as follows:

$$\alpha_i = \Gamma_i + I\sigma_i , \quad (2)$$

where a_i is the decay rate, Γ_i is the effective decay rate and σ_i is the electron collisional rate parameter of the $1s_i$ level which is related to the total electron collisional ionization cross section.

The stored signals from the oscilloscope are treated and analyzed using the least-squares fitting technique. The Levenberg-Marquardt algorithm is used in the least-squares fitting. A set of initial values for parameters (amplitudes, decay rates and τ) are predicted based on an educated guess and previous research. Then the program minimizes the weighted mean square error χ_0^2 by changing the parameters several times until χ_0^2 can get a smaller value (generally, it is in the range of 10^{-7}-10^{-8}).

The weighted mean square error χ_0^2 is given by the relation

$$\chi_0^2 = \frac{\sum_{i=1}^{i_{\max}} [S(t_i, P) - e(t_i)]^2}{N} , \quad (3)$$

$S(t, P)$ is the theoretical prediction from expression (1) at time t using a set of parameters P, $e(t)$ is the experimentally measured signal at time t, and N is the number of data points.

4. RESULTS AND DISCUSSION

In this work, two transitions $1s_3$-$2p_7$ (653.29 nm) and $1s_4$-$2p_8$ (650.65 nm) have been studied. The first transition corresponds to the population excitation from the $1s_3$ metastable state to the $2p_7$ state, which is connected radiatively with all $1s_i$ states. The second transition corresponds to the population excitation from the $1s_4$ semi-metastable state to the $2p_8$ state, which is connected radiatively with $1s_5$, $1s_4$, and $1s_2$ states.

4.1 $1s_3$-$2p_7$ Transition at 653.29 nm

The time resolved OG signals of this transition are recorded for nine different discharge current values from 5 to 13 mA and are shown in Fig. 1. The first peak of the OG signal is positive and is due to an increase in ionization or an increase in current, which caused an increase in the voltage across the ballast resistor. This positive peak then decays to a negative value and returns to the equilibrium with a time scale of the order of microseconds.

Photon excitation from the $1s_3$ state will diminish the metastable atom population (Ne^*) and thereby reduce ionization of neon atoms in the discharge. This excitation will simultaneously enhance the population of $1s_4$ and $1s_2$ levels that, in turn, efficiently radiate to the ground state, so the number of energetic photons rises. Consequently, photoionization of the excited neon states by energetic photons and electron production on the cathode increase. As a result, this laser transition causes an increase in the number of energetic photons in the discharge and depletes the metastable levels.

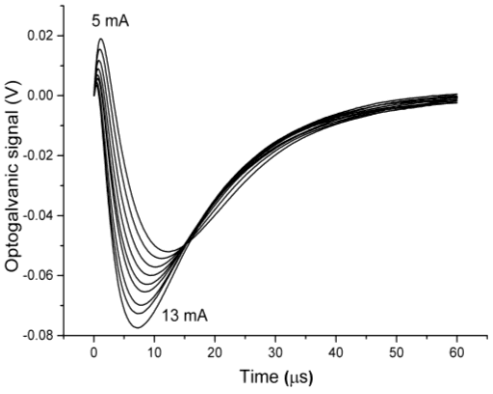

Fig. 1 – Observed time resolved OG signals of the neon transition $1s_3$-$2p_7$ (653.29 nm) for nine different currents (5-13 mA). Each signal is an average of 512 laser pulses

Since the laser beam passes through the discharge in the axial direction, the observed signal is an integral over the OG signals in different regions of the discharge [15]. In each discharge region, a competition between the various mechanisms discussed above occurs, and the behavior of the OG signal of the $1s_3$ to $2p_7$ excitation effectively depends on the initial $1s_3$ population redistribution between the lower $1s_i$ levels and on their decay rates by diverse mechanisms [16]. Comparing the transition probability from $2p_7$ to $1s_i$ manifold, we can notice a high probability of the transition to the $1s_4$ state which, in turn, produces energetic photons and a reasonable probability of transitions to metastable states, while $1s_2$ has the smallest transition probability [17].

As a consequence, we could consider that in the first 2 μs of the observed signal in this work, ionization by energetic photons and electron impact ionization are the dominant mechanisms due to the excess of electrons produced at the cathode by the VUV radiation. After this time, metastable-metastable collisional ionization can take over and become the dominant mechanism, which prompts a negative signal due to the decreasing population of metastable states.

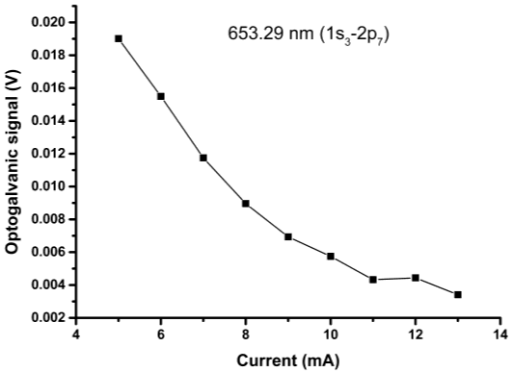

Fig. 2 – Intensity of OG signals of the neon transition $1s_3$-$2p_7$ (653.29 nm) vs. discharge current

The observed shape of the $1s_3$-$2p_7$ OG signal is quite similar to all transitions reported in literature originating from the $1s_3$ or $1s_5$ state [8, 9]. This confirms that all time resolved signals of transitions originating from the $1s_3$ or $1s_5$ state are similar and do not depend on the $2p_j$ states [10].

The OG signals of the transition plotted in Fig. 1 show that the signal amplitude decreases with increasing current, as presented in Fig. 2, which indicates that with an increase in the discharge current, metastable-metastable collisional ionization becomes the dominant mechanism in the discharge.

It was reported that the intensity of the transitions originating from $1s_3$ and $1s_5$ states decreases with increasing current [10]. The same applies to the result shown in our work, as illustrated in Fig. 1. However, we have to mention that Mahmood et al. [9] reported that the $1s_5$-$2p_9$ and $1s_5$-$2p_4$ transitions increase with current, while the $1s_5$-$2p_5$ transition decreases with current. Therefore, the OG intensity behavior with current for transitions originating from $1s_3$ and $1s_5$ states still needs further efforts.

Monte Carlo least squares fitting for these different OG signals is performed using the four terms of expression (1). The behavior of the decay rates with current, as well as their fitting equations, are shown in Fig. 3. They are well expressed by the following linear fitting equations:

$$b = 0.49 + 0.056\,I\,, \tag{4}$$

$$d = 0.04 + 0.0058\,I\,, \tag{5}$$

$$f = 0.027 + 0.0077\,I\,, \tag{6}$$

$$h = 0.027 + 0.0077\,I\,, \tag{7}$$

where b, d, f and h are in μs and the discharge current I is in mA.

From equations (4)-(7), four lifetimes of $1s_i$ levels are found: 2, 25, 33 and 33 μs. Basically, the $2p_7$ state can de-excite to the four $1s_i$ states. As the parameter d is assigned to the negative amplitude (– 1 V), it is concluded that the lifetime of the $1s_3$ state is 25 μs.

The lowest lifetime found from the fit (2 μs) is assigned to the $1s_2$ state because it is a resonant state. The two other lifetimes must be attributed to the $1s_5$ and $1s_4$ states. The three states $1s_3$, $1s_5$ and $1s_4$ show almost similar lifetime in the discharge.

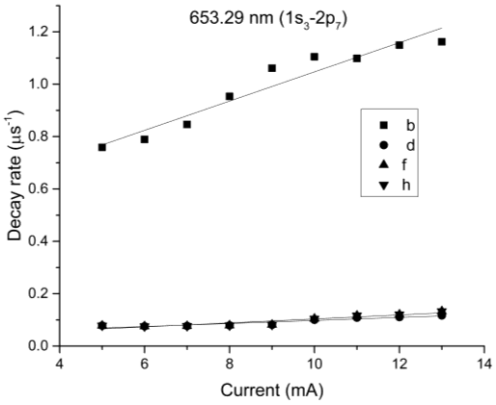

Fig. 3 – Plot of decay rates of the four $1s_i$ states vs. discharge current and their linear fit for the $1s_3$-$2p_7$ neon transition

As shown from Fig. 3, the ratio of the decay rates is $b/d \approx 10$-12. This is expected because the $1s_2$ state is a resonant state which decays faster than other states via VUV radiation, while the ratio of the decay rates of other states is almost equal to 1, so the $1s_{3,4,5}$ states decay at the same rate through different mechanisms.

The amplitude ratios extracted from the fitting parameter values show that the contribution of the $1s_3$ state is the most important in the observed OG signal, the other $1s_i$ states have almost equivalent involvement in the signal.

The obtained effective lifetimes of the $1s_2$ and $1s_4$ states found here are much greater than the radiative lifetimes, which are 1.2 ns and 16 ns, respectively [12]. This can be explained by the radiation trapping mechanism. In this mechanism, the radiation emitted from the $1s_i$ states resulting from de-excitation to the ground state will be partially re-absorbed by another atom, and the fluorescence will be reproduced again. This mechanism makes the effective lifetime of $1s_2$ and $1s_4$ states much longer, and the population will not decay radiatively to the ground state with the same rate.

The shift of the peak with increasing current shown in Fig. 1 matches the expected behavior (towards a shorter time) because this transition $1s_3$-$2p_7$ follows the selection rule $\Delta J = \Delta K = +1$ [9].

4.2 $1s_4$-$2p_8$ Transition at 650.65 nm

The OG signals of this transition are recorded for six different discharge current values from 6 to 11 mA and are presented in Fig. 4. The OG signal consisted of two positive peaks, followed by a decay to equilibrium with a time scale of tens of microseconds. The temporal shape is quite similar to the shape reported by different authors [6, 17].

The signature of the OG signal for the $1s_4$-$2p_8$ excitation effectively depends on the initial population redistribution of the $1s_4$ state between the $1s_i$ levels and on their decay rates. The excited population of the $1s_4$ state is redistributed after de-excitation to $1s_4$ with a large probability, to $1s_5$ and finally to the $1s_2$ state [17]. This population redistribution will increase the population in the $1s_5$ metastable state and slightly increase the population of the $1s_2$ resonance state. Therefore, the observed signal is again an integral over the OG signals in different regions of the discharge [15], where in each region there is competition between the different mechanisms discussed above.

The Monte Carlo least-squares algorithm was used to fit the OG signals of this transition at different discharge currents. An excellent agreement between the experimental and fitted signals is observed.

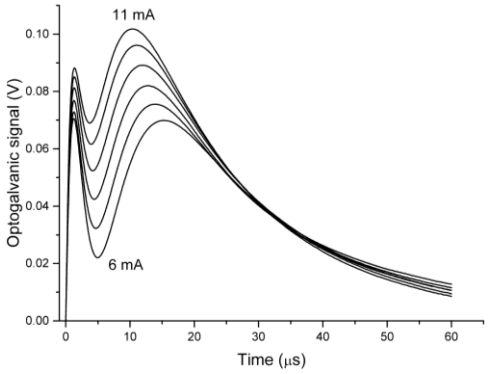

Fig. 4 – Observed time resolved OG signals of the neon transition $1s_4$-$2p_8$ (650.65 nm) for six different currents (6-11 mA). Each signal is an average of 512 laser pulses

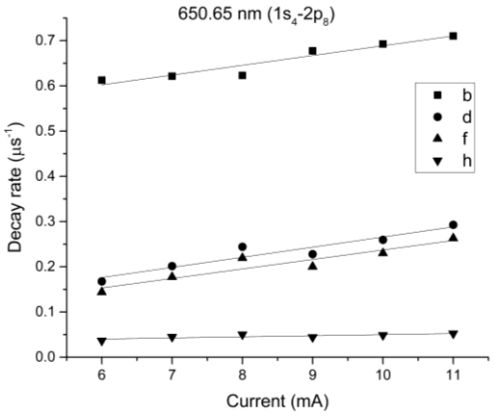

Fig. 5 – Plot of decay rates of the four $1s_i$ states vs. discharge current and their linear fit for the $1s_4$-$2p_8$ neon transition

The negative amplitude c, associated with the decay rate d, correlates with the total decay rate of the initial $1s_4$ state upon excitation to the $2p_8$ level. As demonstrated in Fig. 5, the decay rates b, d, f and h follow a linear relationship with current, as expected from expression (2). So, the effective lifetimes and the electron collisional rate parameters of the $1s_2$, $1s_3$, $1s_4$ and $1s_5$ states could be deduced.

The decay rates are expressed by the following fitted equations:

$$b = 0.47 + 0.022\,\mathrm{I}\,, \tag{8}$$

$$d = 0.042 + 0.022\,\mathrm{I}\,, \tag{9}$$

$$h = 0.025 + 0.0024\,\mathrm{I}\,, \tag{10}$$

$$f = 0.027 + 0.021\,\mathrm{I}\,, \tag{11}$$

where b, d, f and h are in μs and the discharge current I is in mA.

From equation (9), the value of the effective lifetime of the $1s_4$ state is deduced as 24 μs, which is consistent with what was found above for the $1s_3$-$2p_7$ transition.

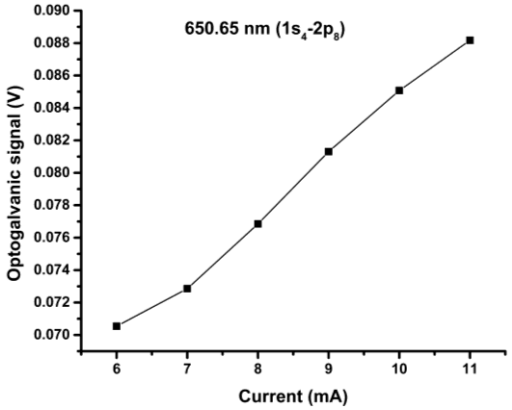

Fig. 6 – Intensity of OG signals of the $1s_4$-$2p_8$ neon transition (650.65 nm) vs. discharge current

This value is much shorter than the radiative lifetime of this state, which is 16 ns [14]. This is attributed again to the radiation trapping effect. The lifetime of the $1s_2$ state is found to be 2 μs. The effective lifetimes extracted from equations (10) and (11) are 37 and 40 μs which are related to the $1s_3$ and $1s_5$ states.

The decay rate ratio extracted from Fig. 5 for the different $1s_i$ states shows that the $1s_2$ state decays faster than other states due to VUV emission, while the $1s_4$ state decays faster than $1s_{3,5}$ due to the same mechanism. It should be noted here that the decay rate of the $1s_3$ and $1s_5$ states is different and the ratio between them is around 4-5. We can explain this behavior by considering that the $2p_8$ state decays only to $1s_5$ and not to $1s_3$, we expect that $1s_5$ takes more time to decay than $1s_3$, and the effective lifetime for the $1s_3$ state is 37 μs and for the $1s_5$ state is 40 μs. The contribution of the $1s_4$ state is the most important in the OG signal. Its amplitude is one order of magnitude more than the smaller participation of the $1s_5$ state. The $1s_3$ state has a larger involvement in the signal than the $1s_2$ state.

Fig. 6 shows that the OG signal increases with current. This behavior is opposite to the behavior shown in ref. [6] corresponding to the $1s_4$-$2p_{10}$ transition. The increasing behavior of intensity with current is consistent with the behavior of the transitions following the selection rule: $\Delta J = \Delta K = +1$ [9]. With increasing current, the first peak shifts towards a longer time, while the second peak – towards a shorter time.

5. CONCLUSIONS

The time-resolved OG signals of the $1s_3$-$2p_7$ and $1s_4$-$2p_8$ transitions are very well fitted by a four-term rate equation model using the Monte Carlo least squares fitting technique. The dominant competing discharge processes are metastable-metastable collisional ionization and ionization by energetic photons for the studied transitions. The effective lifetimes of the different $1s_i$ states for both transitions are coherent, and they are 2 μs for the $1s_2$ state and 25-40 μs for the $1s_3$, $1s_4$, and $1s_5$ states. A four-term equation was useful to get consistent lifetimes for the different $1s_i$ states.

ACKNOWLEDGEMENTS

The authors would like to express their gratitude to the Director General of AECS Prof. I. Othman for his continuous encouragement and support.

REFERENCES

1. Y. Oki, N. Kidera, M. Maeda, *Opt. Commun.* **110**, 105 (1994).
2. K. Alnama, J.-H. Fillion, D. Gauyacq, *Journal of Quantitative Spectroscopy and Radiative Transfer* **105**, 139 (2007).
3. R. Shaw, C. Barshick, L. Jennings, J. Young, J. Ramsey, *Rapid Commun. Mass Spectrometry* **10**, 316 (1996).
4. O. Pirali, D. Tokaryk, *J. Chem. Phys.* **125**, 204308 (2006).
5. P. Misra, I. Misra, X.L. Han, *Nonlinear Analysis: Theory, Methods & Applications* **71**, e661 (2009).
6. N. Piracha, R. Feaver, T. Gilani, R. Ahmed, R. Ali, M. Baig, *Opt. Commun.* **282**, 2532 (2009).
7. X. Han, V. Wisehart, S.E. Conner, M.C. Su, D.L. Monts, *Contrib. Plasm. Phys.* **35**, 439 (1995).
8. X. Han, M. Su, C. Haridass, P. Misra, *J. Mol. Struct.* **695**, 155 (2004).
9. S. Mahmood, M. Anwar-ul-Haq, M. Riaz, M. Baig, *Eur. Phys. J. D* **36**, 1 (2005).
10. N. Piracha, K. Nesbett, S. Marotta, *J. Mol. Struct.* **881**, 1 (2008).
11. G. Racah, *Phys. Rev.* **61**, 537 (1942).
12. A. Sasso, M. Ciocca, E. Arimondo, *JOSA B* **5**, 1484 (1988).
13. C.E. Moore, *Circular of NBS* **467** (1949).
14. A.A. Radzig, B.M. Smirnov, *Reference Data on Atoms, Molecules, and Ions* **31** (1985).
15. G. Guthöhrlein, L. Windholz, *Physics of Ionized Gases, XV International Symposium*, 467 (1995).
16. T. Fujimoto, Y. Uetani, Y. Sato, C. Goto, K. Fukuda, *Opt. Commun.* **47**, 111 (1983).
17. A. Ben-Amar, G. Erez, R. Shuker, *J. Appl. Phys.* **54**, 3688 (1983).

Про оптогальванічну спектроскопію з роздільною здатністю в часі неону у розряді з порожнистим катодом

Koutayba Alnama, Abdulkader Jazmati

Department of Physics, Atomic Energy Commission of Syria, P.O. Box 6091, Damascus, Syria

Оптогальванічні (OG) сигнали з роздільною здатністю в часі переходів $1s_4$-$2p_8$ (650,65 нм) і $1s_3$-$2p_7$ (653,29 нм) досліджено у неоновій плазмі постійного струму. Числова підгонка сигналів на основі моделі рівняння швидкості з чотирьома доданками була використана для з'ясування внеску в сигнал від чотирьох рівнів $1s_i$. Досліджено еволюцію швидкостей розпаду чотирьох станів неону $1s_i$ як функції струму розряду. Домінуючими процесами розряду для першого переходу були фотоіонізація та ударна

іонізація, тоді як для другого переходу – метастабільний-метастабільний механізм іонізації зіткненням був доданий до раніше згаданих механізмів для отримання OG сигналу. Визначено ефективний час життя станів $1s_i$ для обох переходів, який для резонансного стану $1s_2$ становить 2 мкс, а для станів $1s_{3,4,5}$ – 40 мкс. Великий ефективний час життя всіх станів $1s_{2,4}$ у порівнянні з їх радіаційним часом життя пояснюється ефектом захоплення випромінювання. Досліджено внесок станів $1s_i$ в сигнали OG. Участь стану $1s_3$ була найбільш важливою в сигналі переходу $1s_3$-$2p_7$, тоді як стан $1s_4$ має великий внесок у сигнал переходу $1s_4$-$2p_8$.

Ключові слова: Оптогальванічний, Ефективний час життя, Неон, Властивості плазми, Порожнистий катод.